Chapter 4

Self-assembled Nanofibers of Copper Phthalocyanine

This chapter describes a method for producing 1-D organic nanofibers by exploiting intermolecular dispersive forces during the self-assembly of CuPc molecules. The average length of these CuPc nanofibers deposited at 100 °C, a temperature much lower than that for synthesis of carbon nanotubes, was ca. 500 nm, with diameters in the range 15–50 nm. XRD analysis of these nanofibers revealed that they possessed an α phase structure. HRTEM images indicated that the CuPc nanofibers formed through layered stacking of CuPc molecules. These CuPc nanofibers exhibit field emission characteristics (with a turn-on field of 13.6 V/μm) and follow Fowler–Nordheim behavior in a manner similar to that of carbon nanotubes. The stable emission current and relative simplicity of their synthesis suggests a broad range of applications for CuPc nanofibers in nanoscience and nanotechnology.

4.1 Introduction

One-dimensional (1-D) nanostructures of inorganic materials continue to attract a great deal of interest because of their peculiar properties, relative to those of their bulk counterparts, and great potential for application [133–137]. Presently, however, the conditions employed to synthesize such inorganic nanostructures involve the use of high temperatures and/or catalysts. Many recent studies have indicated that organic compounds can form 1-D nanostructures under mild conditions when intermolecular dispersive forces are exploited in self-assembly processes [17, 97-99, 138–140]. When

biased in a vacuum chamber, most of these nanostructures exhibit excellent field emission characteristics [97, 99, 140]. Copper phthalocyanine (CuPc), which has been known for almost a century, is a particularly appealing compound for a variety of applications. For example, its extreme resistance to chemical and thermal degradation and its p-type semiconducting characteristics have led to its use as a hole transport layer in organic light-emitting diodes (OLEDs) [141] and as an active layer in organic thin film transistors (OTFTs) [28]. In addition, the excellent photoconductive properties of CuPc enable its application in the photoconductive layers of photocopying machines and solar cells [31, 142]. All of these applications are based, however, on the electrical characteristics of CuPc in the form of thin films. To our knowledge, there have been no previous reports describing the applications of CuPc as 1-D structures. The planar macrocyclic structure and extended π-electron system of CuPc molecules suggested to us that they would be good candidates for forming 1-D structures through intermolecular π–π stacking interactions. In this study I prepared 1-D CuPc nanofibers and evaluated their field emission characteristics. I have characterized these CuPc nanofibers using scanning electron microscopy (SEM), X-ray diffraction spectroscopy (XRD), and high-resolution transmission electron microscopy (HRTEM) techniques.

4.2 Experimental Section

The CuPc films were grown through vacuum sublimation in a thermal coater at a base pressure of ca. 3×10^{-6} torr. Commercial powders of CuPc ($C_{32}H_{16}CuN_8$; Sigma-Aldrich) were sublimed onto various substrates, including Al, Ti, TiN, Au, and SiO_2, from a heated crucible (ca. 100 °C). The corresponding deposition rate, determined using a quartz crystal microbalance, was ca. 3 Å/s. To study the effect of the temperature on the film morphology, these substrates were maintained at 25, 100, 150, or 200 °C.

Structural investigations were performed using a JEOL JSM-6500F scanning electron microscope. Grazing incident X-ray diffraction was measured using a PHILIPS X'Pert Pro X-ray diffraction system with a Cu-Kα radiation source. Contact angles and surface energies were determined using a KRŰSS GH-100 universal surface tester. The profiles and fine structures of the nanostructures were imaged and analyzed using a JEOL JEM-2010F high-resolution transmission electron microscope equipped with an Oxford

energy dispersive spectrometer. The Raman specra was measured using a Jobin Yvon LABRAM HR Micro-Raman system, the samples were excited by a He-Ne laser (wavelength: 632.8 nm). The field emission measurements were performed in a vacuum chamber (ca. 10^{-6} torr) with a cylindrical copper electrode (diameter: 2.2 mm) positioned above the substrate surface at a distance of 75 μm. A Keithley 237 instrument was used to measure the emission current of the CuPc nanofibers as a function of the sweep bias.

4.3 Results and Discussion

The choice of film growth method and the crystalline properties and surface energies of the substrates have profound effects on the surface morphologies of coated organic thin films [143]. In most cases, the crystallinity of the substrate strongly affects the crystallinity of the deposited film. The surface energy of the substrate, which governs the mobility of the deposited molecules on that surface, determines the wetting ability of the coated film. Therefore, to determine the growth conditions necessary to prepare 1-D CuPc nanostructures, I deposited CuPc molecules onto different substrates, namely Al, Au, Ti, TiN, and SiO_2, at various temperatures and used SEM to investigate their morphologies.

4.3.1 Film morphology

Figures 4-1 (a) and 1(b) present SEM images of CuPc films deposited at room temperature onto SiO_2 and Au substrates, respectively. Both images display contiguous granular crystals that possess smooth morphologies. The mean diameters of the granular crystals formed on the Au and SiO_2 substrate were both ca. 25 nm. Similar granular morphologies were exhibited for the films coated on the other substrates (Al, Ti, and TiN), although with different crystallite sizes. When the substrates were heated above 100 °C, however, I observed totally different morphologies. Figure 4-1 (c) displays the in-plane island morphology of the CuPc layer on SiO_2. In contrast, the layer deposited onto the Au substrate possessed an out-of-plane 1-D nanofiber morphology [Fig. 4-1(d)]. The CuPc packing morphologies on TiN were similar to those on the gold surface, whereas those on the Ti and Al substrates were a mixture of both kinds. The average length of the nanofibers formed on the gold substrate was ca. 500 nm, with their diameters falling in the range 15–50 nm.

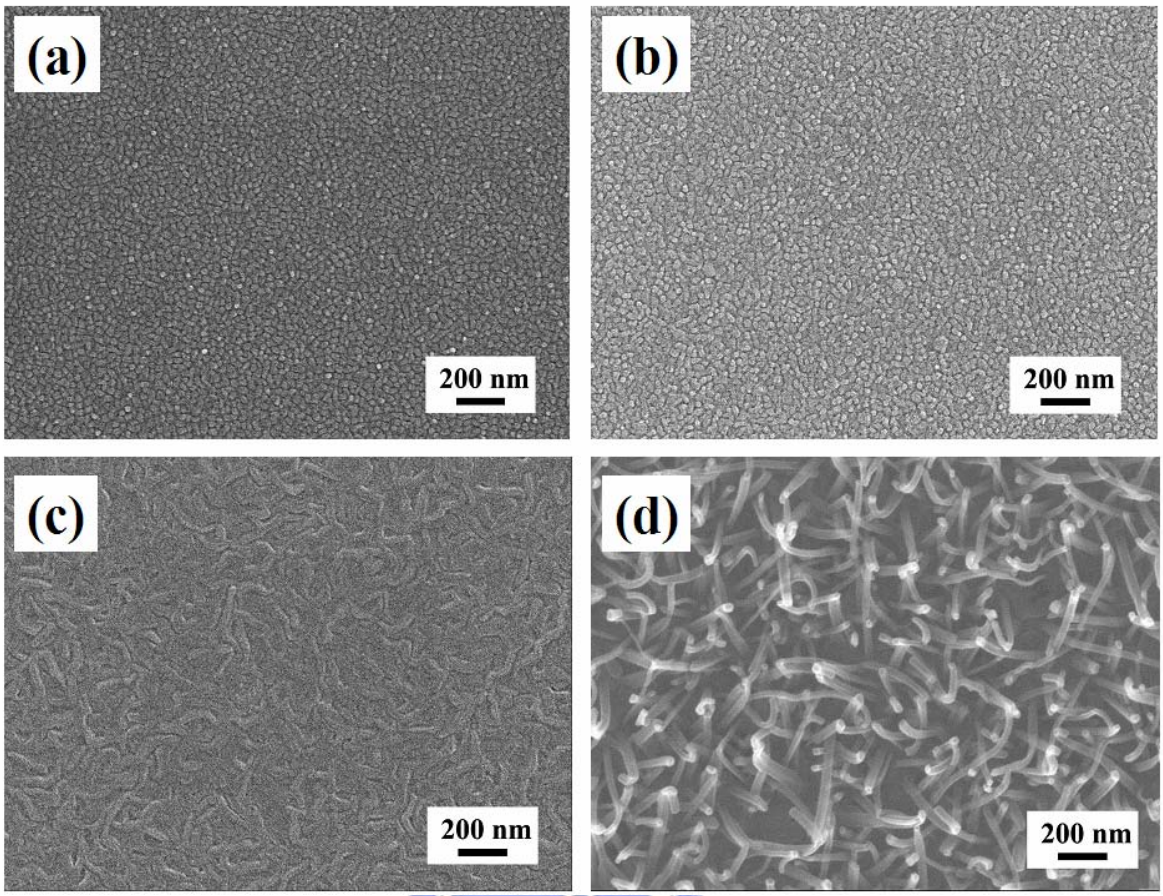

Figure 4-1 *Top-view SEM images of CuPc layers deposited at room temperature on (a) SiO_2 and (b) Au and at 100 °C on (c) SiO_2 and (d) Au.*

At a higher deposition temperature, but with the same process time, the CuPc nanofibers that formed were longer and had larger diameters, but their density was lower. Figure 4-2 displays the various morphologies of the CuPc layers deposited at (a) room temperature and at (b) 100, (c) 150, and (d) 200 °C. For the CuPc nanofibers deposited on the Au surface at 150 °C, the average length increased to 1 μm and the mean diameter expanded to 60 nm. As the substrate temperature increased to 200 °C, the fiber density drops in consequence of some CuPc adsorbates desorbed from the substrate, in addition that high temperature provides more energy to the adsorbates and makes them with higher mobility to diffuse to the energy preference sites.

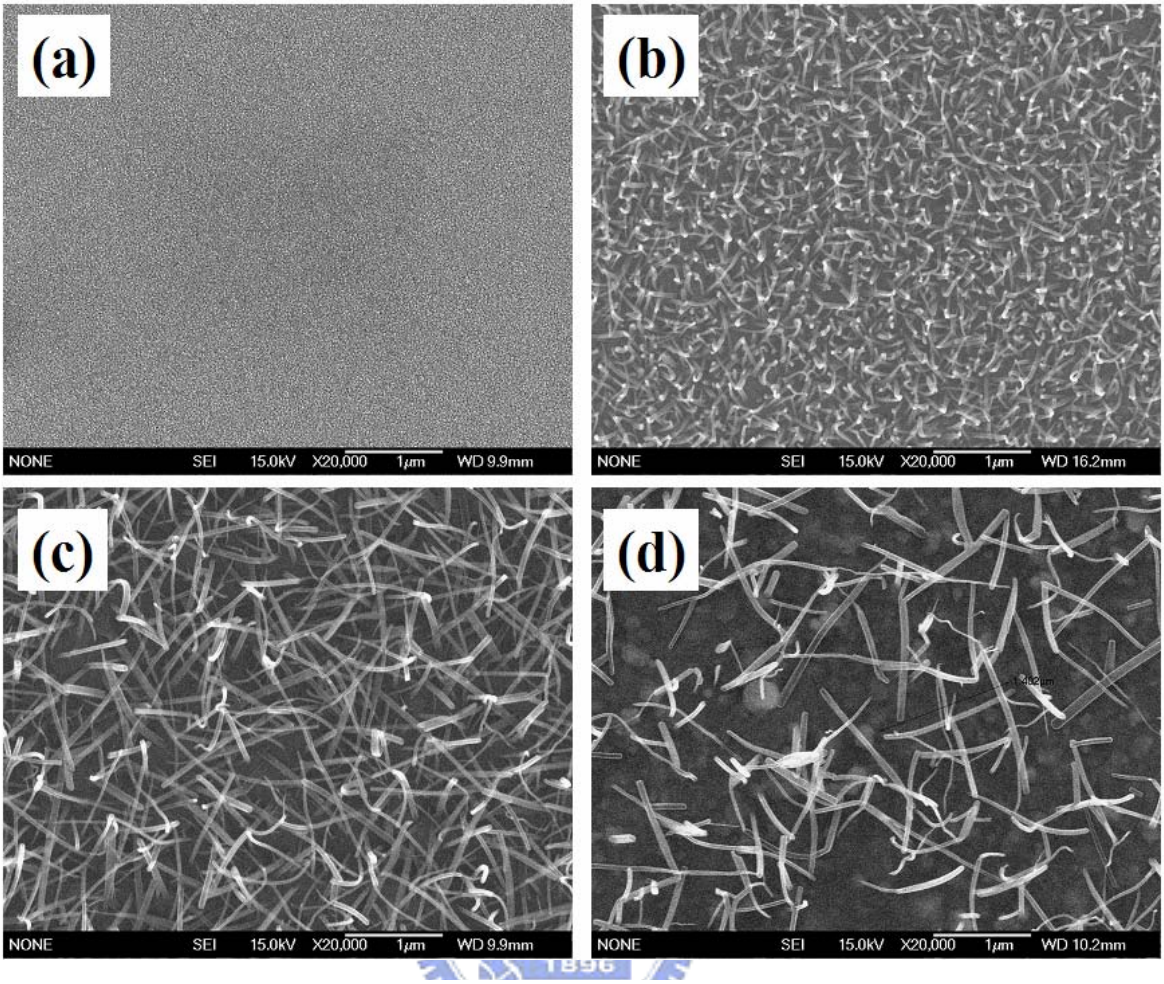

Figure 4-2 *Top-view SEM images of CuPc layers deposited on Au substrates at (a) room temperature and at (b) 100, (c) 150, and (d) 200 °C.*

4.3.2 Surface energy

Contact angle measurements indicate that SiO_2 has a higher surface energy (50.7 mJ/m^2) than does gold (39.4 mJ/m^2), suggesting that the oxide substrate has a higher concentration of unsaturated surface bonds, which tend to adsorb molecules to lower the surface free energy. Therefore, it was not unexpected that the deposited CuPc molecules would have a stronger tendency to cover the whole SiO_2 surface, rather than stack to form out-of-plane nanofibers.

In the case of the CuPc layer formed on the gold substrate, the change in morphology that occurred upon increasing the temperature can be explained by considering the following equation [85]:

$$\gamma = \gamma^0 \left(1 - \frac{T}{T_c}\right)^n \quad (1)$$

where γ is the surface energy at temperature T and γ^0 is the surface energy at the critical temperature, T_c; the value of n may be closer to unity for metals. According to this formula, the surface energy of the gold substrate decreases as the temperature increases. This reduction in surface energy weakens the molecule–substrate interactions, resulting in the intermolecular π–π interactions becoming dominant. Meanwhile, the high substrate temperature favors surface diffusion, driving the adsorbed molecules toward growth at certain nucleation sites, which are formed owing to the lattice mismatch between CuPc and Au polycrystalline. [30, 144] Therefore, the CuPc molecules prefer to stack up into nanofibers, rather than spread out to cover the gold substrate in a mesh-like film.

The surface energies for Ti, Al, and TiN are 37.51, 35.14, and 36.3 mJ/m^2, respectively. These values are similar to—but lower than—the surface energy of the gold substrate. The CuPc layers on those substrates all exhibit the out-of-plane nanofiber morphology, except that a mesh-like morphology coexists on the Al and Ti substrates. Although the lower surface energies should lead to weaker interaction forces between the adsorbate and the substrates, these metal substrates are more easily oxidized than is the gold substrate. I suspect that the oxygen atoms of the resulting metal oxides react, or interact noncovalently, with the organic molecules to cause this phenomenon. For the TiN surface, its relative inertness toward oxygen and columnar crystal morphology combine to form the out-of-plane nanofiber structure.

4.3.3 Crystal phase indentified by GIXRD

Depending on its processing conditions, CuPc may form one, or a mixture, of many crystal phases, which are termed the α, β, γ, δ, ε, and x phases [145]. Of the various polymorphic forms, the most common structures are the α and β phases, which exhibit slightly different structural and electrical characteristics. Films deposited at room temperature exhibit the α phase, whereas those deposited at higher temperatures transform into the β phase [146]. Figures 4-3 (a) and (b) present the grazing incident X-ray diffraction (GID) patterns of the CuPc layers deposited at room temperature and 150 °C, respectively. The incident angle and the scan step used to obtain both patterns were 0.5

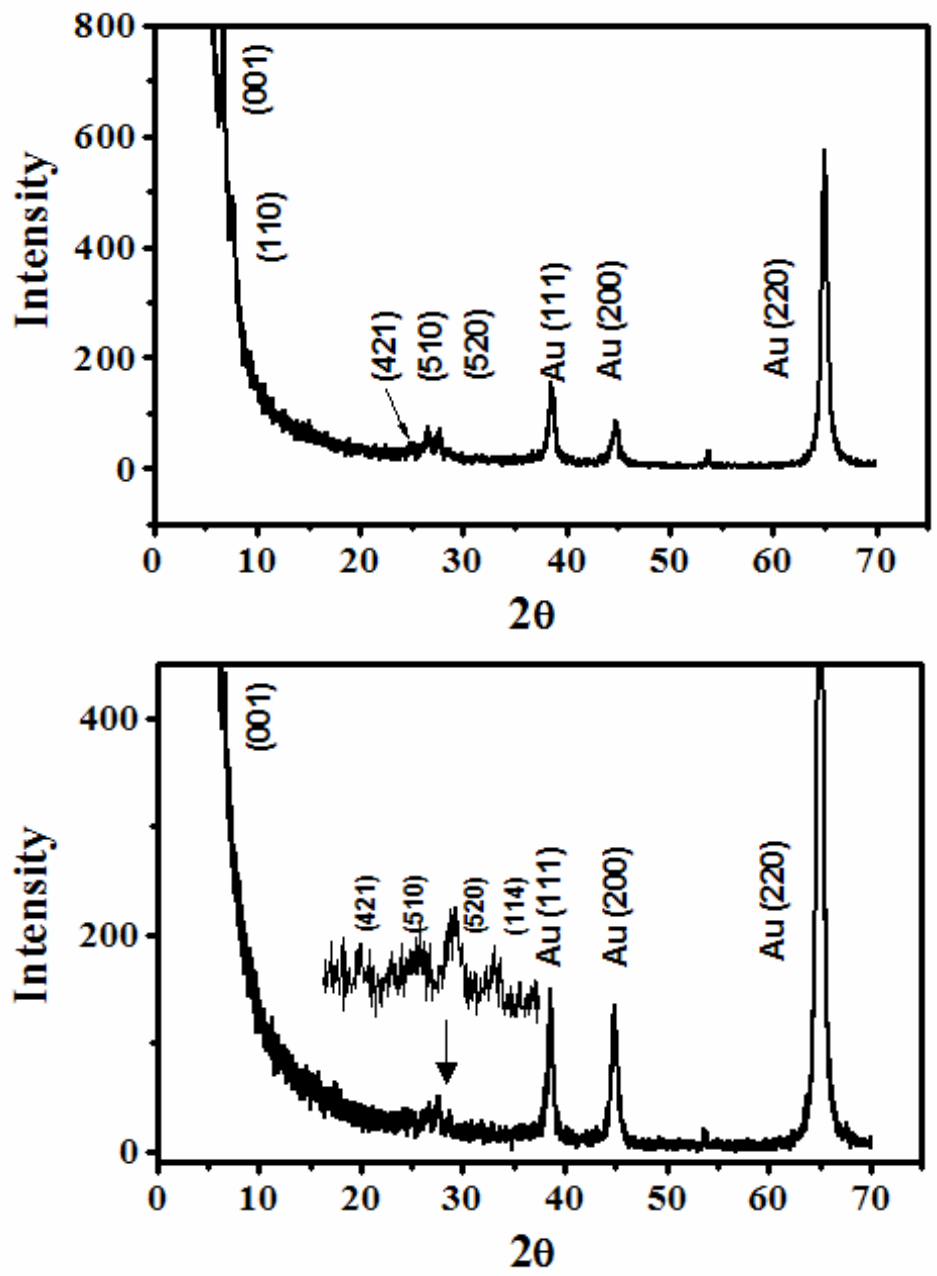

Figure 4-3 *XRD spectra of CuPc layers deposited on Au substrates at (a) room temperature and (b) 150 °C.*

and 0.02°. The 2θ peaks at 38.4, 44.7, and 64.9° in both patterns are associated with the gold substrate. The recognizable diffraction peaks of the CuPc film at (001), (110), (421), (510), and (520) in Figure 4-3 (a) indicate that the CuPc film that I deposited at room temperature existed in the tetragonal α phase [147]. The diffraction peaks from the CuPc nanofibers deposited at 150 °C [Fig. 4-3 (b)] are similar to those arising from the CuPc film, but the (110) peak is absent. Although, in theory, the crystallinity of a film should

be greater after higher-temperature processing, the morphology change (from a film to fibers) at the higher deposition temperature resulted in a rough and discontinuous CuPc layer on the gold substrate, leading to lower intensities of some of the diffraction peaks. According to the reference diffraction peak for a monoclinic β-phase structure [147], at least three intense peaks should be present at 7.0, 9.2, and 23.8°. These peaks are absent in Fig. 4-3 (b), suggesting that the structure of the CuPc nanofibers deposited at 150 °C was that of the α phase.

4.3.4 Crystal phase indentified by Raman spectrometer

The CuPc is a planar molecule consisting of 57 atoms and possessing D_{4h} point group symmetry, as shown in Figure 4-4. This planar molecule has the following vibrational representation

$$\Gamma_{vib} = 14A_{1g} + 13A_{2g} + 14B_{1g} + 14B_{2g} + 13E_g + 6A_{1u} + 8A_{2u} + 7B_{1u} + 7B_{2u} + 28E_u$$

where A_{1g}, B_{1g}, B_{2g}, and E_g modes are Raman active [148]. The nondegenerate A_{1g}, B_{1g} and B_{2g} modes are in-plane vibrations, and double degenerate E_g is out-of-plane vibrations. In the case of B_{1g} modes, the atomic shift is a symmetric relative to the twofold axis C'_2 through the central copper atom Cu, and the benzene rings. In the case of B_{2g} modes, the atoms are shifted symmetrically relative to the C''_2 axis through the N_α and N_β atoms. The symmetry of molecular vibrations can be determined from the analysis of the polarized Raman spectra of the oriented CuPc layers grown on a substrate. The characteristc peaks and their relavant positon as well as interpretations are summarized in Table 1 [149]. Since CuPc films possess polymorphic forms, i.e. α and β phases, which exhibit slightly different structural as deposited at various temperatures, I further used the Raman spectra to indentify the film structure of those samples deposited at different temperature. Figure 4-5 shows the Raman spectra of CuPc films deposited at various temperatures. However, it shows no distinct difference among the CuPc films deposited at room temperature, 100 °C and 150 °C. Therefore, the phase of the CuPc film did not alter a lot under a process temperature of 150 °C. This result is consistent with the previous discusson of GIXRD.

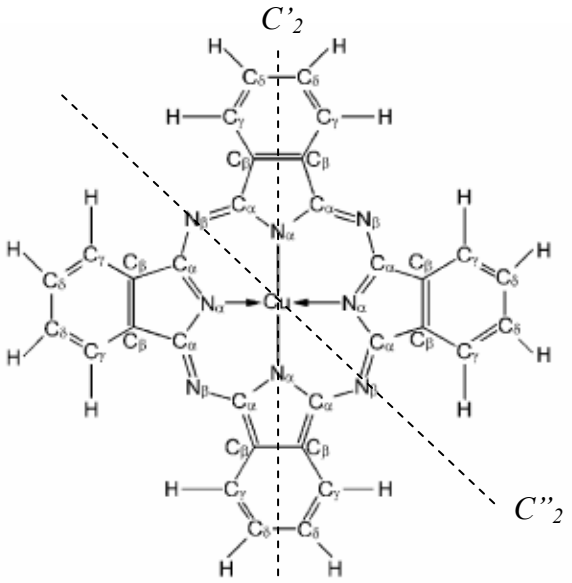

Figure 4-4 *The molecular structure and atomic notation of CuPc molecule [148].*

Table 4-1 *Raman peak parameters of α- and β-phase CuPc thin film. The corresponding interpretation is also listed in the table [149].*

α phase CuPc	β pahse CuPc	Interpretation
Peak Position (cm^{-1})	Peak Position (cm^{-1})	
171.1 (w)	173.4 (s)	Isoindole in-phase
234.5 (s)	236 (w)	Cu-N stretch
254.7 (w)	255.4 (w)	
591 (m)	590 (s)	Isoindole ring deformation
684 (m)	681 (s)	16 mimbered inner ring breathing
839 (m)	833 (m)	C-N stretching (aza groups)
1010 (s)	1010 (s)	Isoindole in-plane bending
1041 (m)	1040 (w)	C-H bending -Isoindole group
1109 (m)	1104 (s)	C-H bending -out of plane
1338 (m)	1339 (m)	C_α-C_β stretch-pyrrole group
1414 (m)	1409 (s)	C-N stretch-pyrrole group
1527 (w)	1523 (w)	C_β-C_β stretch-pyrrole group
1589 (m)	1586 (w)	
1610 (m)	1608 (s)	

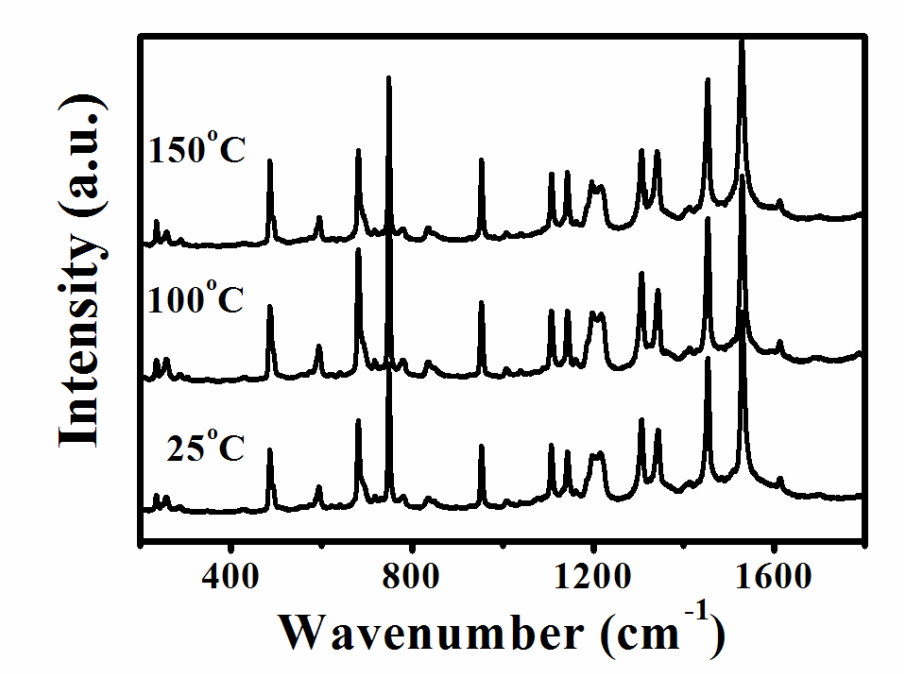

Figure 4-5 *The Raman spectra of CuPc films deposited at 25 °C, 100 °C and 150 °C, respectively.*

4.3.5 HRTEM

Fig. 4-6 (a) presents an HRTEM image of a single CuPc nanofiber (diameter: 16 nm), which was synthesized on a heated gold substrate (100 °C). Unlike related carbon nanotubes (CNTs), no catalyst appears at the top of the fiber. This feature was further verified after recording the energy dispersive spectra (EDS), which exhibited no peaks arising from gold atoms at any point along the entire length of the CuPc nanofiber. Fig. 4-6 (b) presents a magnified image of the CuPc nanofiber; it exhibits fringes, suggesting that the CuPc units were stacked in the growth direction and aligned in a parallel manner. This high-resolution image indicates that the nanofibers formed through layered stacking of CuPc molecules. Fig. 4-6 (b) also presents the corresponding profile analyzed using Fuji Imagegauge software. The average interlayer distance (4.3 Å) slightly exceeds the value of 3.8 Å found for the spacing h between two molecular layers along the stacking direction of α-CuPc thin films [150], depicted schematically in Fig. 4-6 (c). This difference may be caused by the high aspect ratio of the 1-D nanofiber structure, which suffers more stress and has a larger inclination angle (φ') of stacking than that angle (φ) of 2-D smooth thin film structures. Therefore, at a constant interlayer distance d (3.4 Å), a larger inclination angle (φ') corresponds to a greater distance h, according to the cosine relationship.

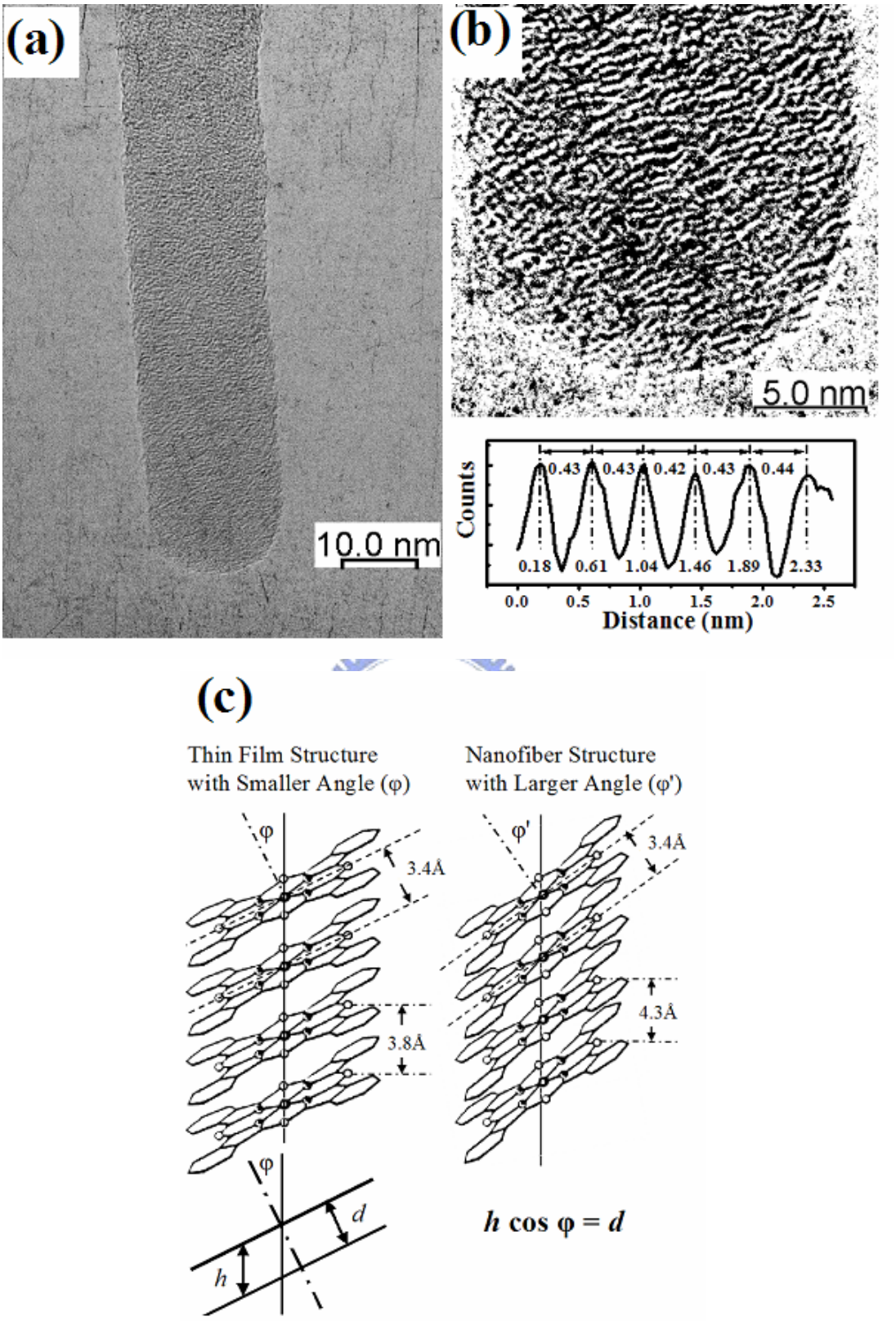

Figure 4-6 *(a) HRTEM image of a single CuPc nanofiber (diameter: 16 nm). (b) Magnified image of this nanofiber, which has been over-contrasted to intensify the fringes, and the corresponding profile analyzed using Fuji Imagegauge software. (c) Schematic illustration of CuPc molecules stacked at different inclination angles (φ).*

4.3.6 Field emission of CuPc nanofibers film

I performed field emission characterization of the CuPc nanofibers that I synthesized on a heated (100 °C) gold substrate; this analysis was performed under vacuum (5×10^{-6} torr) after placing a cylindrical Cu electrode (diameter: 2.2 mm) 75 μm above the surface of the sample. The Cu electrode was connected to the source monitor unit (SMU) of a Keithley 237 instrument; the gold substrate under the CuPc nanofibers was grounded. Figure 4-7 presents a plot of the emission current density J as a function of the applied field E. The turn-on field required for the CuPc nanofibers to produce a current density of 10 μA/cm^2 was 13.6 V/μm, a value that is somewhat higher than the fields required for turning on other previously reported organic nanofibers [97, 99, 140]. The electron affinity (3.1 eV) of CuPc [151] is much lower than the work function (5.1 eV) of the gold substrate, so the energy barrier (ca. 2 eV) that exists at the metal–organic contact limits electron injection from the substrate. Consequently, the finite injected electrons require a higher electric field to reach the same level of emission current. The inset of Fig. 4-7 displays a plot of ln (J/E^2) as a function of $1/E$; this straight line implies that the field emission from these nanofibers follows the Fowler–Nordheim (FN) theory [104, 152–153]. Taking into account the work function of bulk CuPc (3.1 eV), I deduced the field enhancement factor β of the CuPc nanofibers from the slope of the FN plot to be ca. 130. Normally, the enhancement factor is proportional to the length-to-radius ratio (L/r) of a 1-D nanostructure [97]. Because the CuPc nanofibers reported herein possess shorter lengths (500 nm) and larger radii (50 nm), it is reasonable that they would exhibit a smaller enhancement factor relative to those of AlQ_3 organic nanowires [97].

Figure 4-8 displays the emission current stability of the CuPc nanofibers when biased at 1000 V (E = 13.3 V/μm) for 1800 s. The mean current density was ca. 3 μA/cm^2, with a perturbation within one order of magnitude, which may arise from the random orientation of the CuPc nanofibers on the surface. The field emission current did not decay during the period of the stability measurement, suggesting that these CuPc organic nanofibers are suitable for use in electron emitting devices.

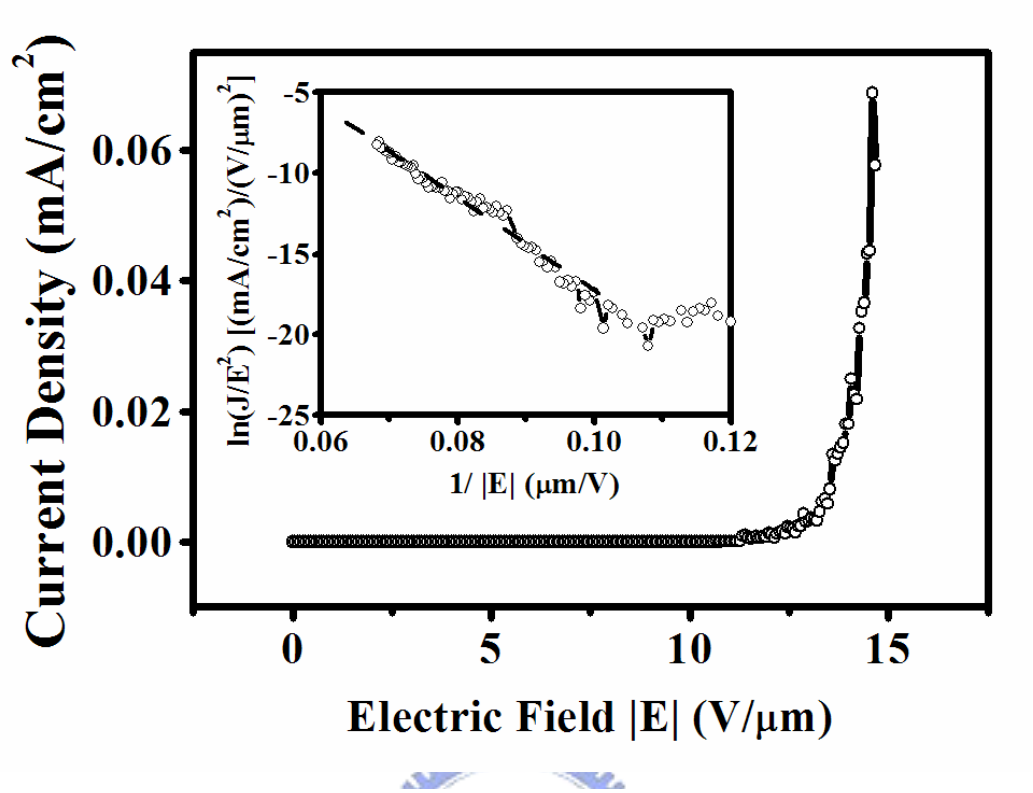

Figure 4-7 *Field emission J–E curve of the CuPc nanofibers. Inset: Corresponding FN plot.*

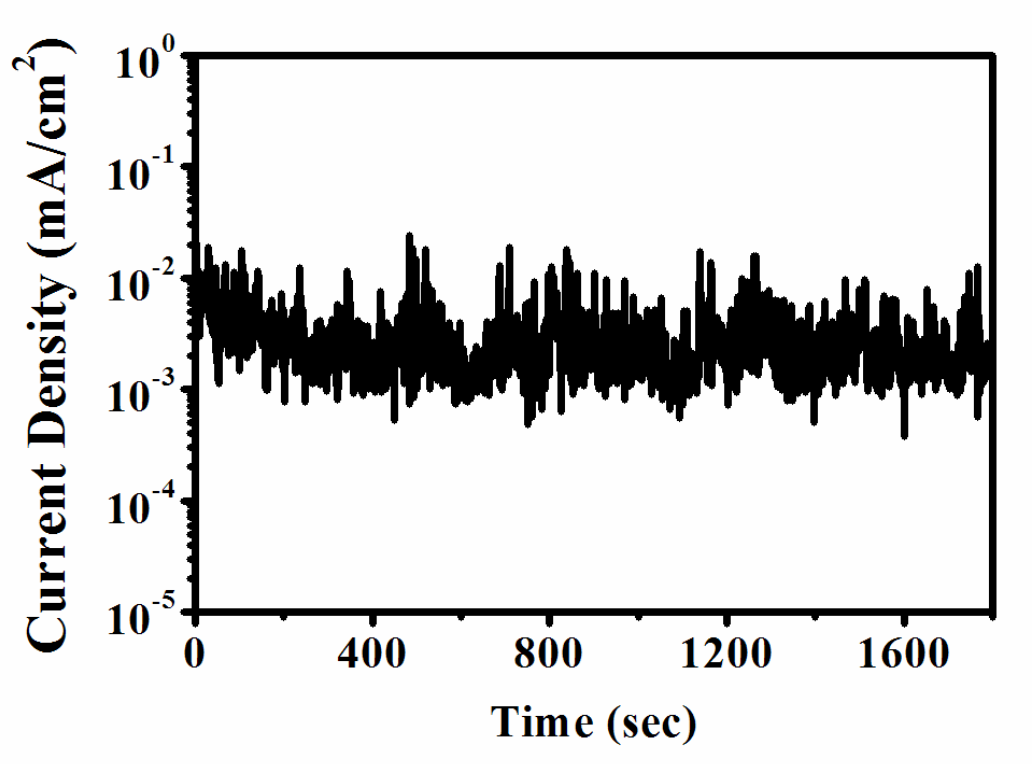

Figure 4-8 *Emission current stability of the CuPc nanofibers at constant voltage.*

4.4 Conclusions

In this paper, I describe a simple method for producing CuPc organic nanofibers at low temperature. XRD analysis of these nanofibers revealed that they possessed α-phase structures; HRTEM images indicated that they formed through layered stacking of CuPc molecules. The CuPc nanofibers exhibit field emission characteristics and follow Fowler–Nordheim behavior similar to that of CNTs. The stability of the emission current and the simplicity of the synthetic process suggest that these CuPc nanofibers may find a broad range of applications in nanoscience and nanotechnology.